Chem Soc Rev

This article was published as part of the

From microfluidic application to nanofluidic phenomena issue

Reviewing the latest advances in microfluidic and nanofluidic research

Guest Editors Professors Albert van den Berg, Harold Craighead and Peidong Yang

Please take a look at the issue 3 table of contents to access other reviews in this themed issue

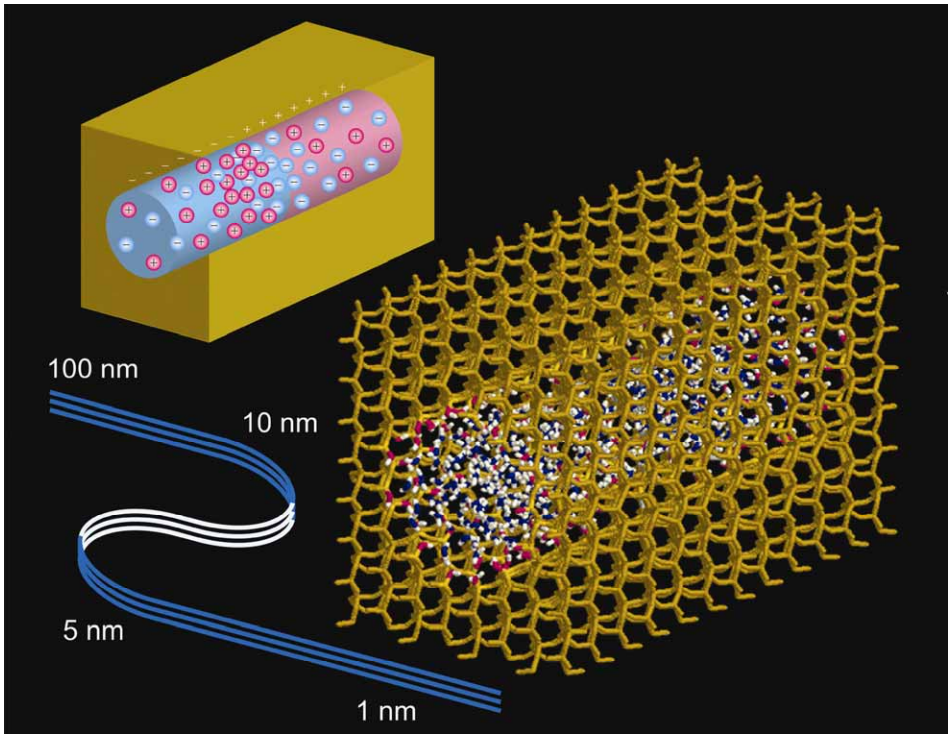

Continuous separation of cells and particles in microfluidic systems†

Andreas Lenshof and Thomas Laurell

Received 4th November 2009
First published as an Advance Article on the web 4th February 2010
DOI: 10.1039/b915999c

The progress in microfabrication and lab-on-a-chip technologies has been a major area of development for new approaches to bioanalytics and integrated concepts for cell biology. Fundamental advances in the development of elastomer based microfluidics have been driving factors for making microfluidic technology available to a larger scientific community in the past years. In line with this, microfluidic separation of cells and particles is currently developing rapidly where key areas of interest are found in designing lab-on-a-chip systems that offer controlled microenvironments for studies of fundamental cell biology. More recently industrial interests are seen in the development of micro chip based flow cytometry technology both for preclinical research and clinical diagnostics. This *critical review* outlines the most recent developments in microfluidic technology for cell and particle separation in continuous flow based systems. (130 references)

Introduction

Microfluidics is inherently a domain where high performance cell and particle handling has proven to be very successful. Some of the ruling technology platforms, which are industrial and clinical standards for high quality cell processing, are found in the fluorescence activated cell sorter (FACS) and in the Coulter Counter. The FACS technology was pioneered by Leonard Herzenberg and co-workers[1,2] at Stanford in the late 1960-ies, rendering him the Kyoto Prize in 2006. The importance of the FACS technology in modern biological and medical research cannot be stressed enough. The key feature of the FACS is that the sample flow is performed in a sheath flow mode, where the cell suspension is coaxially laminated in the centre of a buffer flow. By precise design of the sheath flow conduits and by very accurate control of the two flow rates, a highly laminar flow condition with eddy free fluidics is obtained. This yields a precise and reproducible spatial location of the cells in the fluid core and thus precision optics can be employed for high speed detection of cells as they pass along the sheath core. The combination of fluorescently labelled cell

Dept. Measurement Technology and Industrial Electrical Engineering, Div. Nanobiotechnology, Lund University, 22100 Lund, Sweden. E-mail: andreas.lenshof@elmat.lth.se, thomas.laurell@elmat.lth.se
† Part of the themed issue: From microfluidic application to nanofluidic phenomena.

Andreas Lenshof

Andreas Lenshof (né Nilsson) is currently a Post Doc at the Laurell Group at Lund University. He received his PhD at Lund University in 2009. He has been working with acoustic microfluidic systems for the last 10 years in both academia and industry. His research is currently focused on acoustic particle and cell manipulation in biomedical applications. He has received several national innovation awards, including the SKAPA award 2003.

Thomas Laurell

Professor Thomas Laurell holds a position as Professor in Medical and Chemical Microsensors and has since 1995 built his research activities around microtechnologies in biomedicine (http://www.elmat.lth.se/forskning/nanobiotechnology_and_labonachip). Laurell recently started a new applied nanoproteomics laboratory at the Biomedical Centre in Lund, integrating microfluidics and nanobiotechnology developments with medical research. This research is focused on new microchip technologies in the area of biomedicine, biochemistry, nanobiotechnology with a focus on disease biomarkers, diagnostic microsystems and miniaturised sample processing. Laurell also leads the clinically oriented research environment CellCARE, (www.cellcare.lth.se), which targets chip based cell separation utilising ultrasonic standing wave technology (acoustophoresis) as the fundamental mode of separation.

specific antibodies and the FACS technique opened the route to a revolution in modern cell biology.[3] Current instrumentation offers analysis rates in the range of 10 000–20 000 cells per second and with readout from at least 8 different wavelengths. Likewise, the Coulter Counter is characterized by laminar flow conditions as cells in a sample suspension are aspirated through a micro orifice while the change in impedance is monitored as the cell displaces the reference buffer in the orifice.[4] The impedance change is then correlated to an average diameter of the cell and each impedance change over a set threshold is registered as a cell count. The Coulter Counter has become a real work horse in the clinical field and is used in everyday analyses, *i.e.* blood components.

These are both good examples of very successful applications of microfluidics to cell based monitoring where microscale and laminar flow conditions have been key to the success in real life applications. The lab-on-a-chip community has consequently also tried to realise the corresponding concepts in the chip based planar technology offered by microfabrication. Numerous approaches to coulter counting chip devices have been reported[5,6] and more recently simultaneous impedance monitoring at multiple frequencies has been employed to increase the ability of the devices to also perform cell speciation.[7,8]

Likewise chip integrated FACS devices with a multitude of technical approaches to the sorting mechanism have been reported where *e.g.* the Quake group reported fluorescence activated electroosmotic flow switching.[9] Fluorescence activated hydrodynamic cell switching was later reported by Kruger *et al.*[10] and Wang *et al.*[11] and more recently the Morgan group demonstrated a chip integrated flow cytometer that utilised dielectrophoretic forces to focus the cells into the channel centre for confocal readout.[12] Both Coulter Counter and fluorescence activated detection techniques can be employed to chip integrated continuous flow based cell sorting where the specific sorting step is implemented by employing an external force to the targeted cell. Although very high separation efficiencies can be accomplished in these modes of operation the system throughput is generally lower as every single cell is analysed and based on readout an individual separation event is executed. This should be compared to cell separators that operate on the direct differential physical properties of each cell category, which perform the separation in a continuous flow bulk process. The microfluidics field has consequently also proposed numerous approaches where the intrinsic physical properties compose the key parameters for separation. This opens the field for label free differentiation which is a key issue for many applications in clinical medicine.

With the rapid development in the lab-on-a-chip area, new microfluidic solutions to cell handling, processing and monitoring is now also emerging at an increasing pace.[13] The ability to design advanced microfluidic networks in combination with both actuation and sensing/monitoring is driving novel concepts for advanced on chip cell studies as well as new means to capture/retain,[14] separate and/or concentrate cell species from complex biofluids. Current developments in cell separation and cell enrichment encompass both the employment of physical forces from external sources or forces induced on the cells by controlled hydrodynamics.[15] In order to enable improved separation performance or targeted sub-speciation of cells, magnetic nanoparticle labelling have been realised and are today in clinical use within transfusion medicine where magnetic bead labelled leukocyte separation is performed at a preparative level (not primarily benefitting from the microfluidic domain) for the treatment of hematological disorders.[16,17] The magnetic nanoparticle labelling allows magnetic forces to act only on cells that express specific cell surface markers and enables enrichment or depletion of targeted cells from large sample volumes in *e.g.* autologous blood processing. The MACS (magnetic activated cell sorting) based cell separation can be regarded as a trapping based technique and is thus bound to be run in a batch mode. Several other cell trapping techniques have also been proposed in the literature to enable detailed studies of cells at single or few cell levels. This area was recently reviewed by Nilsson *et al.*[14] and trapping techniques integrated in microfluidic systems are thus not incorporated herein.

This review overviews the most recent developments in continuous flow based cell and particle separation and manipulation. Separation is accomplished by the intrinsic physical properties of a cell type, which defines a specific finger print that can be expressed as an induced force that drives the separation of cells in complex mixtures. A key is the microscale domain, which provides inherent benefits for accuracy in the separation. Microfluidic systems using externally induced forces such as dielectric, magnetic, acoustic and optical are described as well as lab-on-a-chip systems for cell separation where hydrodynamic effects are capitalised upon to obtain separation based on *e.g.* inertial forces, pinched flow effects or deterministic lateral displacement.

Active separation using external fields

SPLITT—Split thin flow fractionation

One of the earliest microfluidic particle separation methods is the Field Flow Fractionation (FFF), invented by Giddings.[18] This is a generic method where an externally applied field of actuation can be electrically,[19] thermally,[20] gravitationally[21] or cross flow[22] induced for example. The microscale was utilised in the direction of the applied field. The rate of motion of the influenced particle depends on the physical parameters of the particle in relation to the interaction of the applied field and the parabolic flow profile. The mechanism behind the separation depends on the size of the suspended particle, for instance particles approaching the dimensions of macromolecules will be more affected by Brownian motion than larger ones and will therefore display different distribution profiles in the flow profile, Fig. 1. The separation of the different components is determined by the retention time in the separator, thus particle fractionation will occur as the particles will exit the separator at various times which means that the FFF is actually *not* a continuous separation method but rather a flow injection based separation. It is however a very versatile technique which can be used in wide range of separation applications including fractionation of proteins,[23] polymers[24] cells and viruses[25] and its close relation to the continuous SPLITT systems below justifies the mention of the FFF.

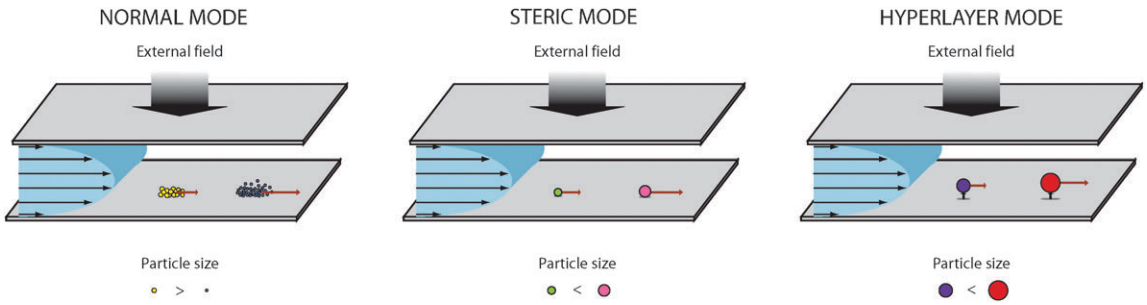

Fig. 1 The different modes of Field Flow Fractionation, *i.e.* normal mode,[26] steric mode[27] and hyperlayer mode.[28] The *normal mode* encompasses submicron particles and macromolecules. The external force drives them toward the wall opposite the side of the incident force where an accumulation of particles and macromolecules will occur. The increased particle concentration by the wall is however counteracted by Brownian diffusion in the opposite direction of the force. The macromolecules, which are smaller in size than the submicron particles, will be more affected by the Brownian motion and move further away from the accumulation wall. Because of the parabolic flow profile, the macromolecules will thus exit the separator before the submicron particles. The *steric mode* FFF acts on larger particles differently than in the normal mode, typical particle sizes of 0.5–10 μm. These particles are too large to be affected by the weak Brownian diffusion counter effect. Instead, the particles will form a thin layer close to the accumulation wall. The larger particles will protrude out of this layer into faster streamlines and exit the separator faster than the small particles that are caught in slower streamlines close to the wall. As this is the opposite result of the normal mode FFF, it is sometimes referred to as reversed mode. The residence time for the steric mode depends only on the size of the particle. For larger particles, >10 μm, the contact with the wall is very limited. Instead they are affected by an opposed force generated by hydrodynamic lift forces that moves them away from the wall. As they are moved a distance greater than their diameter, the retention mode is called *hyperlayer*. The separation in the field is still reversed, that is larger particles first, but the separation does not entirely rely on size but also on other physical properties of the particle such as shape and deformability.

A system closely related to FFF is the split-flow lateral-transport thin (SPLITT) separation cells, also pioneered by Giddings.[29] SPLITT also involves an external force field acting perpendicular to the flow direction, Fig. 2. However, it has an extra inlet with a carrier stream besides the feed stream. The inlet split prevents the two inlet streams from coming in contact with each other until they are under the influence of the external force field. The force affects some particles more than others and they are thus transferred into the carrier medium. The outlet split divides the streams into two outlets collecting the separated sample fractions. The SPLITT is in many ways the role model of particle separation as it is a generic platform containing an arbitrary applied force field and contains flow splitters to divert the fractionated flow streams. Many microfluidic devices have since then proven successful in applying the fundamental design of the SPLITT using magnetic,[30] dielectrophoretic,[31] gravitational[32] and acoustic forces.[33]

Magnetophoresis

Separation by applying an external magnetic field, or magnetophoresis, is done using either a permanent magnet or electromagnets. The magnetic force on a particle with a volume V_p is given by eqn (1):

$$F_{\mathrm{mag}} = \frac{\Delta\chi \cdot V_p}{\mu_0} \cdot (\nabla B) \cdot B \qquad (1)$$

where B is the magnetic flux density, ∇B is the gradient of the externally applied magnetic field, μ_0 is permeability of vacuum and $\Delta\chi$ is the difference in susceptibility between the particle and the fluid. In a homogeneous field with, the net force on a magnetic particle is zero.

Depending of the size of the particle or the magnetic core of a coated particle, the behaviour in the magnetic field differs between nanoparticles and microparticles. Nanoparticles

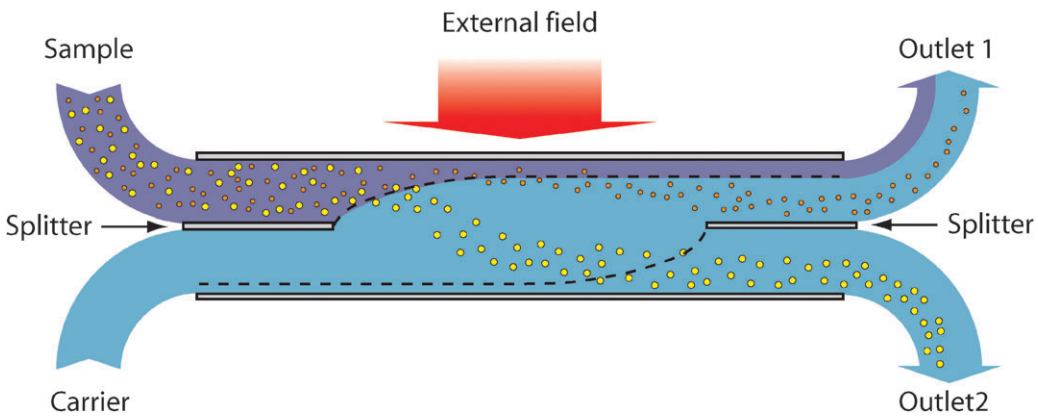

Fig. 2 The principle of split flow thin (SPLITT) fractionation. A particle mix enters from a sample. As they enter the fractionation chamber they are affected by the external force field. The yellow particles are more affected than the smaller orange particles. The force and the flows are tuned such that the more affected particles travel past the flow splitter and are separated from the smaller orange particles.

display no hysteresis in the magnetic field, hence when the magnetic field is turned off they show no remanence and they redisperse in the suspension. In contrast, microparticles display magnetic hysteresis which causes them to agglomerate into clusters.[34] The nanoparticles are therefore preferable since they enable an on/off action of the magnetic interaction, which may be advantageous if several analytical steps are required for a process sequence. Magnetic particles are commonly used in affinity applications where the magnetic particles are coated with a substance that enables specific binding to a desired cell or protein. The combination of simple effective binding and separation has made them very desirable in the biomedical field.[35]

Continuous separation by means of magnetophoresis has been studied widely. Pamme *et al.* reported a continuous magnetophoretic system, where multiple bifurcations provided inlets for buffer solution and a sample inlet at the bottom of the chamber, Fig. 3.[36] The suspended magnetic particles were separated according to size in the separation chamber as particles with the largest volume were affected the most by the magnetic force and subsequently ended up in an outlet closer to the magnet. By utilizing the same device but introducing different reagent buffers in layers, it is possible to perform multi-step biochemical processes on the magnetic particles as they move through the different buffer layers under the influence of the magnetic force.[37] Carr *et al.* used a similar setup where the magnetic field was also applied perpendicular to the flow, but with a chamber that had the possibility to collect 25 different output fractions.[38]

By utilizing particles of different sizes and distinct saturation magnetization, it is possible to separate multiple targets with magnetic tags into separate fractions simultaneously. Adams *et al.* thus enabled separation of two different targets into separate fractions from non-targeted cells using micro-fabricated ferromagnetic strips of various designs in a flow channel.[39] Ferromagnetic nickel strips was also used by Lou *et al.* where magnetic beads with immobilized target proteins, which selectively bind to specific aptamers, were separated from unbound sample *via* flow splitters.[40] Yung *et al.* used the magnetic force to clean blood from fungi contamination during sepsis by having magnetic beads bind to the fungi and transfer the contamination into a parallel waste fluid in a laminar flow system.[41]

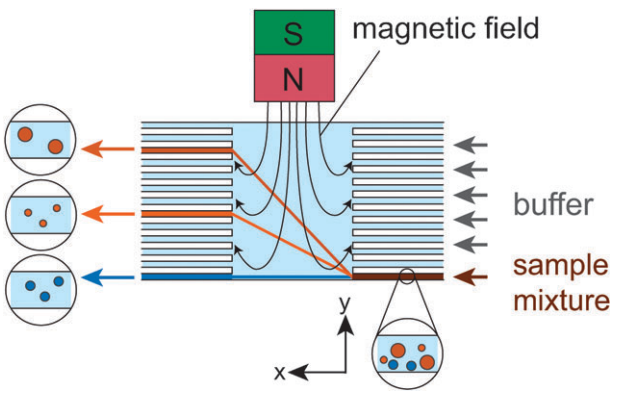

Fig. 3 Magnetophoresis according to Pamme *et al.*[36] Sample suspension enters the separation chamber at the lower right and the particles will be displaced orthogonal to the flow in the upward direction by the magnetic force into the carrier buffer solution and separated. Reprinted with permission from Pamme *et al.*[36] Copyright 2004 American Chemical Society

The magnetic force is not only used to manipulate magnetic particles or magnetically labelled cells which are magnetic or paramagnetic, but also non-magnetic (diamagnetic) objects can be affected as they show a weak repelling force to the magnetic field.[42] This was utilized by Furlani for separating white blood cells (WBC) from red blood cells (RBC) using magnetic forces.[43] This was possible since WBC behave as diamagnetic microparticles while RBC are either para-magnetic or diamagnetic depending on the oxygenation state. Blood cell separation was also performed by Han and Frazier where they included a ferromagnetic wire in the direction of the fluidic flow.[44] The wire caused a high gradient in the magnetic flux which enhanced the magnetic separation and separated WBC from RBC.

By employing a magnetic susceptibility gradient across a microfluidic channel, it is possible to separate particles which otherwise have similar diamagnetic susceptibility and would be difficult to separate.[45] However, isomagnetophoresis enhances the mobility distinction under the susceptibility gradient of the surroundings, and particles migrate and stop at the net position where the susceptibility of particles and the surroundings are equal.

Optical methods

Optical methods, *i.e.* the use of lasers to affect cells and particles, have developed much over the recent years. Early work demonstrated trapping of cells and particles in optical fields, *i.e.* optical tweezers. More recently optical methods have been developed to sort particles in continuous flow based mode as well.

Optical tweezers enable trapping and translation of particles and cells by precise control of a focused laser beam. The principle was first reported by Ashkin in the early 1970's where particles of micron size were accelerated and trapped into optical potential wells.[46] Objects of high refractive index were attracted toward the centre of the beam and propelled away in the direction of the beam. Using two counter propagating beams, he was able to trap particles in three dimensions. Ashkin later developed what became known as optical trapping where dielectric particles were to be trapped and held stable in three dimensions using a single focused beam of light.[47]

The method operates with a Gaussian beam profile and utilizes the fact that there is a very strong electric field gradient in the narrowest part of a focused beam of light, known as the waist of the beam. When a particle enters the beam boundary, it will experience a net force towards the centre of the beam because the larger optical momentum change towards the centre of the beam, see Fig. 4. Less intense beams will pass on a smaller momentum change away from the centre, however, the net momentum will move the particle to the centre where an equilibrium is met and thereby it will be trapped.[48,49] By using infrared lasers, Ashkin *et al.* were able to perform damage-free trapping and manipulation of red blood cells and

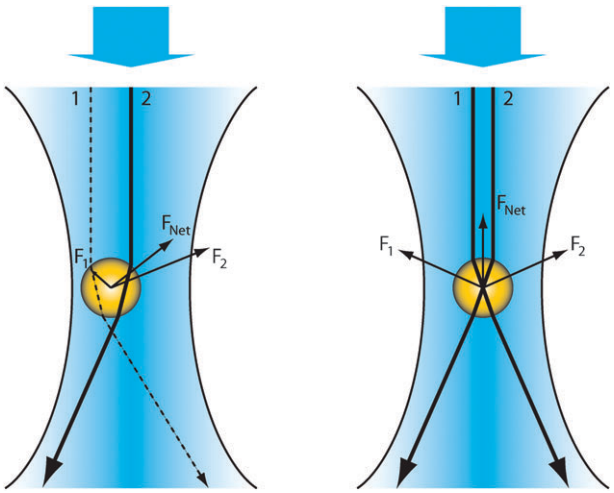

Fig. 4 The principle of optical tweezers. A particle will experience a net force towards the centre of the beam because the more intense part of the beams transfer a larger momentum change towards the centre of the beam.

organelles located within living cells since the haemoglobin and chlorophyll absorption is reduced in the IR spectra.[50]

Optical forces can be used to sort particles in many ways.[52] A way of actively sorting particles is to use the optical force in a similar way as the electrostatic field forces droplets to deflect in a FACS. However instead of using an electrical field to sort particles inside droplets, a laser is activated at the occurrence of a rare event pushing the desired particle out of trajectory into a sorted fraction. This technique has been used by Wang *et al.* for sorting mammalian cells[11] and by Perroud *et al.* for sorting macrophages.[53]

Passive optical sorting have been developed by MacDonald *et al.*[51] An array of laser beams was arranged as an optical lattice through which a flow channel passed for a continuous particle fractionation system. The lattice is a three dimensional structure which enables sorting of particles through a three-dimensional flow. When a flow of mixed particles passes through the lattice, the selected particles are deflected from their original trajectories while the non selected pass on, see Fig. 5. The selectivity depends on the particles sensitivity to the optical potential. The result of the optical lattice will be similar

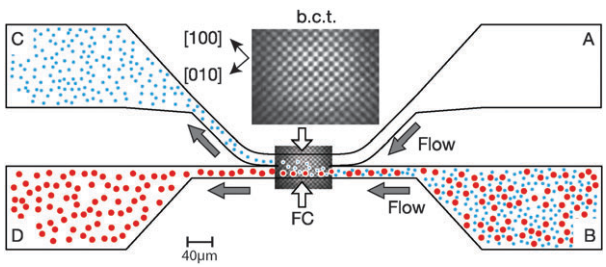

Fig. 5 The concept of optical fractionation presented by MacDonald *et al.*[51] The array of laser beams causes particles to be repeatedly deflected towards the centre of a laser beam. Since the optical force is lower than the Stoke's drag, and the particles display a sideways trajectory dependent of the size and optical properties of each particle, a separation is obtained. Reprinted by permission from Macmillan Publishers Ltd: Nature,[51] copyright 2003

to the deterministic lateral displacement system (described below), with the exception that there will be no physical obstacles, which could be subject to clogging. Ladavac *et al.* showed a similar device in two dimensions using twelve discrete lasers.[54]

Dielectrophoresis

Dielectrophoresis, or DEP, was first investigated by Herbert Pohl in the 1950s.[55] In DEP, a force is exerted on a dielectric particle in a non-uniform electric field. All particles are affected more or less in the presence of an electrical field, and the force does not require the particle itself to be charged.[56] The strength of the force depends on the medium and the particle's electrical properties, on the shape and size of the particle and the frequency of the electrical field.

The DEP force on a homogenous sphere with the radius r can be expressed as:

$$F_{DEP} = 2\pi r^3 \varepsilon_m \mathrm{Re}(f_{CM}) \nabla E_{\mathrm{rms}}^2 \quad (2)$$

where ∇ is the del vector operator and E_{rms} is the root mean square of the applied electric field. $\mathrm{Re}(f_{\mathrm{CM}})$ refers to the real component of the Clausius–Mossotti factor:

$$f_{CM} = \frac{\varepsilon_p^* - \varepsilon_m^*}{\varepsilon_p^* + 2\varepsilon_m^*} \quad (3)$$

where ε_p^* and ε_m^* are the complex permittivity of the particle and the medium. The complex dielectric constant is:

$$\varepsilon^* = \varepsilon - \frac{j\sigma}{\omega} \quad (4)$$

where ε is the dielectric constant, j is $\sqrt{-1}$, σ is the conductivity and ω is the angular frequency of the applied electric field.

By varying the frequency of the applied voltage, it is possible to induce a dipole moment in a particle and thereby cause the particle to experience a movement. Particles having higher permeability than the surrounding fluid, $f_{\mathrm{CM}} > 0$, move to a region of stronger electric field *i.e.* the electrodes, and is called positive dielectrophoresis (pDEP). The opposite occurs when the particles have lower permeability than the fluid, in which case the particles are repelled from the electrodes and is consequently called negative dielectrophoresis (nDEP), see Fig. 6. For continuous fractionation pDEP is not recommended since particles are attracted toward the electrodes and the direct interaction may alter electrode characteristics as well as affect cell activation.[57] Less stress to the cells is also induced at the field minima. Fiedler *et al.* have used nDEP to create virtual flow channels with "channel walls" created by activating the electrodes.[57] They have also used transients to temporarily switch off "the walls" in order to move particles between the flow channels. The choice of frequency is also of great importance as various DEP phenomena only occur at certain frequencies.[58] Wang *et al.* for instance used inter-digitated sidewall electrodes at dual frequencies to separate objects with different dielectric properties.[59]

For the DEP to be functional, a non-uniform electric field is required. One way is to use electrodes of various shapes and designs.[60] Another is to apply voltage along a channel that contains insulating obstacles such as posts[61] or ridges.[62] The electric field becomes non-uniform close to these objects, and

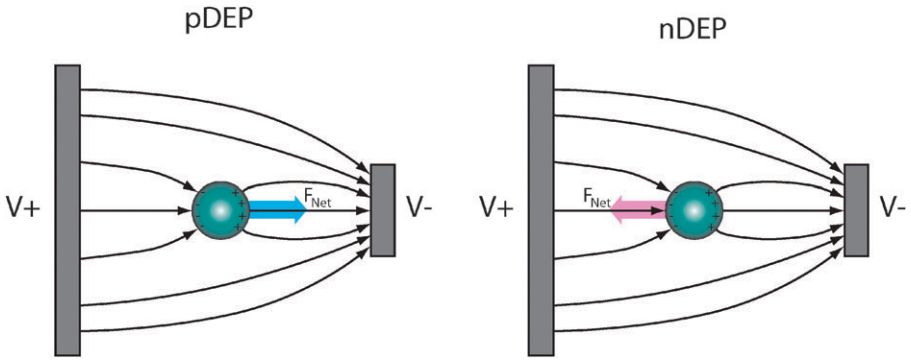

Fig. 6 In pDEP, the dielectrophoretic force moves the object towards the higher electric field and in nDEP towards the lower electric field.

particles flowing around them will be affected by the DEP force. DEP forces do not depend on the polarity of the electric field but rather the field gradient and either AC or DC or both[63] can be used in contrast to regular electrophoresis which uses DC only.

The dielectrophoretic force scales with the volume of the particle, which makes DEP very suitable for size fractionation. Kim *et al*. presented a paper in which multiple cell types were targeted by dielectrophoretic labels of different sizes.[64] Two areas with slanted electrodes at different angles provide the dielectrophoretic force, Fig. 7. The largest beads are affected first and deflect into a buffer flow and line up against the opposite channel wall. The medium sized beads are not deflected by electrode set A because the DEP force is not sufficiently high to counter the hydrodynamic force by the flow. Instead they are deflected by the second set of electrodes and are placed in the middle of the channel. The smallest sized beads are basically unaffected and stay in the sample flow. The size dependency was also utilized by Pommer *et al*. were they separated platelets from whole blood, as the small platelets were less affected than the larger cellular content.[65] However, Cui *et al*. showed that it is possible to reverse the order of separation, *i.e*. eluting the larger particles while retaining the smaller, by pulsing the DEP force in time.[66]

Vahey and Voldman performed DEP in a channel which contained a conductivity gradient.[67] The conductivity gradient was established using a diffusive mixer previous to sample introduction. They managed to simultaneously resolve three types of submicrometer polystyrene beads according to their surface conductance, as well as yeast cells upon membrane integrity.

A particle concentrator was designed by Gadish *et al*. in which the particles are attracted by a pDEP field and are trapped.[68] As the DEP force is deactivated the particles flow with the laminar flow into a concentrated sheet. The concentrator was enhanced with a chaotic herringbone mixer to increase the rate at which the particles come within the vicinity of the DEP force field and thereby the trapping rate increases.

Doh *et al*. separated viable from non-viable yeast cells using DEP.[69] The frequency and the conductivity of the medium were tuned such that the viable cells had a positive response to

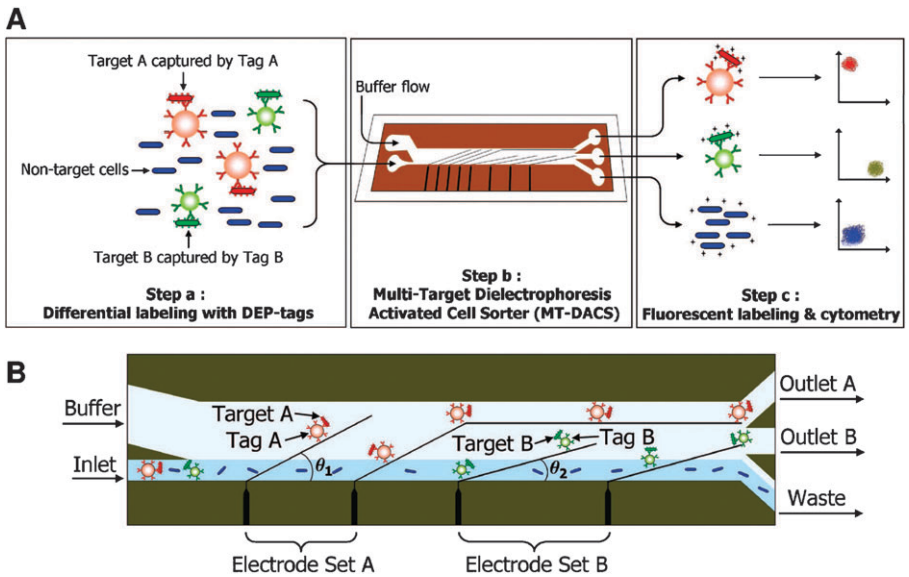

Fig. 7 Multiple target cells flow into the separator *via* the inlet. Target A cells are separated by electrode set A and exit through outlet A. Target B cells are separated by electrode set B and exit through outlet B while non-targeted cells are unaffected and exit through the waste outlet. Target B cells are not deflected by electrode set A because the DEP force is not high enough to counter the hydrodynamic force by the flow. Reprinted with permission from Kim *et al*.[64] Copyright 2008 American Chemical Society.

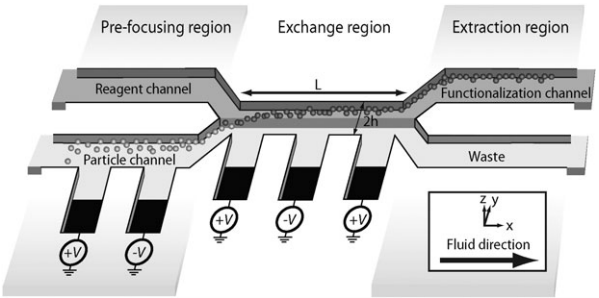

Fig. 8 Particles were prefocused in the particle channel to line up close to the fluidic boundary. They were then switched into the functionalization chamber where they reacted with a reagent. Another chip linked to the functionalization channel pushed the particles back into a clean buffer completing the exchange. From Tornay *et al.*[71] Reproduced by permission of the Royal Society of Chemistry.

the dielectric force and the non-viable had a negative response. The electrode pattern at the bottom of the channel guided the cell fractions to a designated outlet in the continuous flow system. Viability sorting has also been performed by Braschler *et al.*, which used a channel with electrodes operated at different frequencies opposing each other.[70] The particles were focused toward different equilibrium positions depending on their dielectric response. The device was also successfully tested on erythrocytes infected with *B. bovis*, where the infected cells yielded a change in dielectric response as compared to the non-infected cells.

A particle exchanger was presented by Tornay *et al.*[71] The device was designed as a SPLITT, and consisted of two inlets, which merged into a single channel at which the particle transfer occurred and the flows were then again split into two outlet channels, Fig. 8. The particles in the sample channel were first prefocused against the wall closest to the reagent channel by another array of electrodes. When dielectric particles flowed along the electrode array they were subjected to dielectrophoresis forcing them towards the reagent. Because of the laminar flow the particles followed the functionalization channel which was then linked to another chip. This chip, which worked in a similar way, pushed the particles back into a clean buffer solution from the fragment solution thus completing the exchange cycle.

Acoustophoresis

A suspended particle in a standing wave field will experience a radiation force which moves the particle either to a pressure node or to an *anti* node depending on the physical properties of the particle.[72] The force is proportional to the square of the pressure amplitude p_0 and the volume of the particle V_p and inversely proportional to the wavelength λ. The density of the medium and particles are denoted ρ_f and ρ_p, respectively and the corresponding compressibilities β_f and β_p.

$$F_r = -\left(\frac{\pi p_0^2 V_p \beta_f}{2\lambda}\right) \cdot \phi(\beta,\rho) \cdot \sin(2kx) \qquad (5)$$

$$\phi = \frac{5\rho_p - 2\rho_f}{2\rho_p + \rho_f} - \frac{\beta_p}{\beta_f} \qquad (6)$$

The term ϕ in eqn (6) represents the acoustic contrast factor which contains physical properties of the medium and the particle. The sign of ϕ governs the direction of which the particles are moved by the acoustic radiation force, *i.e.* a negative contrast factor moves the particle to the pressure node and a positive towards the *anti* node. Thus, if two particle types of sign shifted acoustic contrast factors are present, a separation of the two will occur.[73] Generally, rigid particles and most cells have a negative contrast factor and will be moved to the pressure node while air bubble and lipid vesicles will gather at the *anti* nodes. The gathering of particles in a node, for instance, will be present at the entire channel height,[74] unless there is a two dimensional focusing in a channel of square cross-section or multiple frequencies in use.[75] By applying an acoustic standing wave of a half wave length, a pressure node is located in the middle of the channel and *anti* nodes at the walls. Because of the laminar flow present in the microchannel, the particles which have reached equilibrium due to acoustic interaction will remain in their lateral position and bands of particles will form. This enables a very easy mode of separation by flow splitters, where particles in the middle of the channel will continue straight forward and the particles close to the walls will exit to the sides.[76] As the entire chip is affected by the acoustic resonance, it is tempting to presume that an even force field prevails in the separation channel. This is however not the case, instead there are several pinching regions where the acoustic force is particularly strong.[77] As the particles follow the flow in and out of these pinching regions, the overall effect is integrated and the visual appearance is that there is an equal force on the particles throughout the acoustically activated channel. It has previously been reasoned that vertical walls have been of paramount importance to accomplish the resonant criteria, but it has recently been shown that this is not the case.[74] The rounded and slanted profile received when wet etching isotropically in glass, has proven to work equally well as anisotropically wet etched silicon channels. This was demonstrated by confocal imaging of the focused particle band as obtained in anisotropically etched silicon channels and isotropically etched glass channels, Fig. 9.

The previously described half wave length separator works well for concentrating particles.[76,78] This was recently utilised in a reverse set-up, depleting cells from whole blood to produce blood plasma as described by Lenshof *et al.*[79] The plasmapheresis chip was constructed to process samples with high cell concentration, *i.e.* whole blood, to deliver high grade cell free blood plasma of diagnostic quality. The separation channel was elongated in a meander type fashion to affect the cells during a longer time to the acoustic field and thereby focus the cells more densely in the channel centre. Extra outlets, located in the centre of the channel bottom removed already acoustically focused cells with a minimum of plasma loss, gradually lowering the cell concentration until cell free plasma was received. The plasma fraction was subsequently linked to a porous silicon sandwich antibody microarray chip for prostate specific antigen detection.

Separating particles or cells with different acoustic contrast factors are the most ideal way of acoustic separation. Erythrocytes and lipid particles have opposite contrast factor

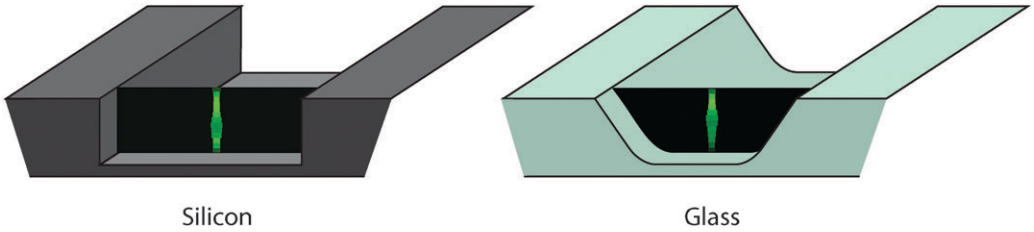

Fig. 9 Confocal cross-section images of acoustophoretically focused fluorescent microbeads in an anisotropically etched silicon channel (left) and an isotropically etched glass channel (right).[74]

signs and thus direct the particles in opposite direction whereby good separation results easily can be obtained.[73,80] However, having a slightly adhesive substance like lipid vesicles forced to the channel side wall in the pressure antinode is far from ideal as they sometimes adhere to the wall, which serves as a seed site for building a lipid stenosis in the channel. This behaviour may cause disturbances in the flow profile which is not desirable. Grenvall *et al*. however solved the problem by introducing a multi node standing wave.[81] The system, which was designed for raw milk preconditioning prior to protein and lipid content analysis, included protective sheath flows and multi node standing waves which prevented lipid particles from coming in contact with the channel walls.

The fact that the radiation force is size dependent was utilized by Petersson *et al*. as they explored the ultrasonic standing wave to size fractionate particles in a device with three inlets and four outlets.[82] In the device, sample with mixed particle sizes enters the separation channel from inlets placed at the side walls of the channel. The same fluid, but without particles, enter the channel through a single centre inlet occupying most of the channel width. As the flow propagates, the particles become affected by the acoustic standing wave present between the channel walls. The largest particles will reach the pressure node located in the centre of the channel first followed by the second largest *etc*. By balancing the flows, such that only the largest particles just reach the centre position before the flow splitter, a particle size gradient can be created, see Fig. 10. The largest particles thereby exit through the centre outlet, and the second largest through the next *etc*. because of the laminar flow profile.

Petersson *et al*. also showed that it is possible to separate particles that normally are acoustically inseparable by altering the density of the carrier medium. A suspension of erythrocytes and platelets showed to be equally affected by the acoustic radiation force. However, by adding caesium chloride to the medium, the medium density increased and resulted in a much weaker force on the platelets and slightly weaker force on the erythrocytes. This resulted in an almost complete separation of platelets and erythrocytes.

An ultrasonic standing wave system for rare event sorting, an acoustic FACS (AFACS), was developed by Grenvall *et al*. where the sorting mechanism was based on a cell specific activation of an acoustic force.[75] The AFACS device was constructed in three sections comprising (1) a hydrodynamic focusing step to line up the sample close to one of the channel walls. (2) a 2-dimensional acoustic focusing at 5 MHz was utilized in order to concentrate the cells away from the channel boundary and align the cells in a flow segment with constant

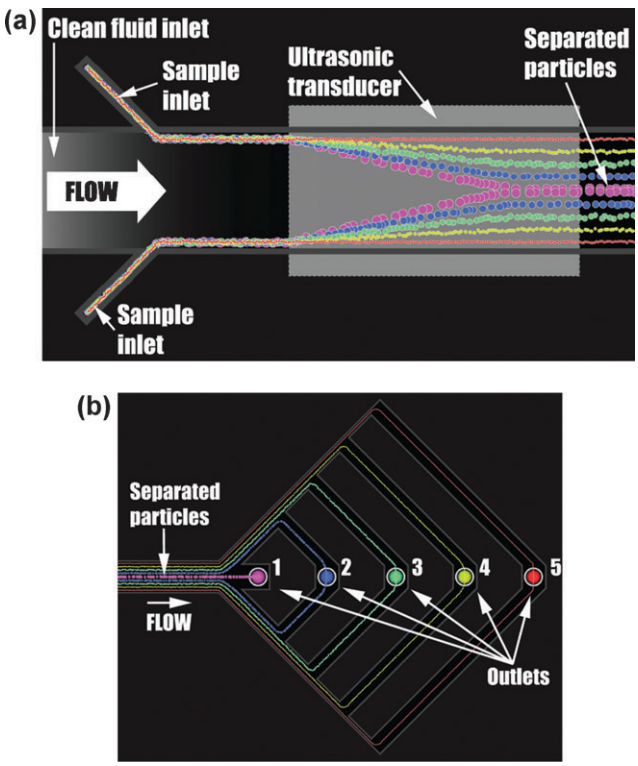

Fig. 10 (a) Particle suspension entering at the sides of the channel. Pink particles are the largest and will thus reach the pressure node first. By adjusting the acoustic force such that only the pink particles reach the node before the multiplex output, fractionation is enabled. Reprinted with permission from Petersson *et al*.[82] Copyright 2007 American Chemical Society. (b) Fractionation of the particle sizes. The largest particles exit through 1, second largest through exit no. 2 *etc*. Reprinted with permission from Petersson *et al*.[82] Copyright 2007 American Chemical Society.

velocity, and (3) the cell sorting section, utilized a standing wave of 2 MHz to acoustically switch cells from the position close to the wall into the centre of the channel which was routed to a different outlet for the selected cell. Separation speeds of 50 switchings per second were reported for the first prototype system. Although displaying modest cell switching rates the AFACS sorting method is expected to be gentle to the cells and thus important applications in clinical cells handling may emerge.[83–85]

A different approach to an acoustically driven FACS was developed by Johansson *et al*.[86] It resembles a commercial FACS in the sense that it affects the fluid surrounding the particle rather than the particle itself. This result in much

longer particle displacement distances (700 μm) compared to a direct particle actuation which is limited to move between a node and an antinode (35 μm) at 10 MHz. A sheath flow of higher density was introduced along one channel wall and the acoustic radiation force acting on the density interface caused a fluidic movement where the particles or cells on either side of the fluid interface were displaced in a direction perpendicular to the standing wave direction. The reported sorting speed was approximately 3 particles s^{-1}.

Laminar flow microchannels offer the possibility to laminate different liquid media in a streaming system. This, combined with acoustic particle manipulation, can be utilized to move particles from one suspending medium to another using acoustic standing waves.[33,87] By adding two extra inlets on each side of the original central inlet, it is possible to move particles from the medium streams on the side into the central, particle-free medium thus exchanging the medium the particles are suspended in. This can be of importance in applications where a more rigorous wash of particles or cells is required and can be considered as the standard unit operation of centrifugation and buffer exchange, performed in many cell assays.

The medium exchange procedure was first illustrated by translation of 5 μm polyamide beads in a buffer contaminated by Evans blue into a clean medium.[87] About 95% of the contaminant was removed in this experiment while it should be mentioned that the level of contamination was quite low. If medium or higher degrees of contamination were used the cleaning efficiency will decrease, probably due to weakly absorbed contaminants on the bead surface or by tailing effects of the beads dragging contaminants with them into the clean buffer. The medium exchange efficiency mentioned above was also repeated with erythrocytes in saline solution and Evans blue as pollutant.

An enhanced medium exchange chip with two integrated acoustic buffer exchange units in sequence was presented by

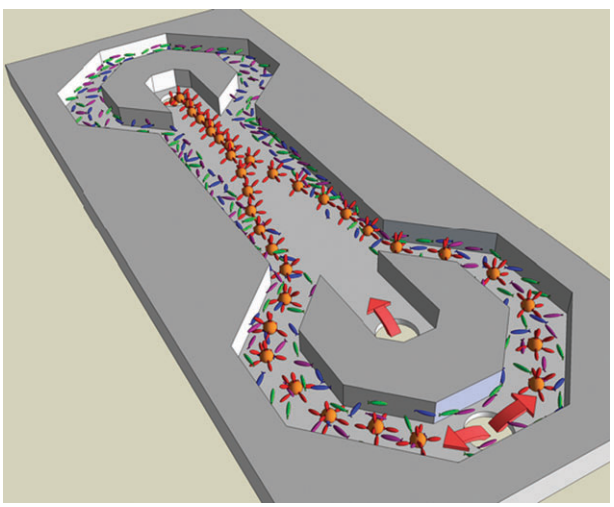

Fig. 11 Acoustic affinity specific extraction of phage particles from phage display libraries.[89] Microbeads coated with a selected antigen were used to extract phages with a specific binding for the targeted antigen from a vast library of bacteriophages. Acoustic forces pulled the antigen beads with bound bacteriophages from the complex bead/phage library mixture into the clean buffer in the channel centre.

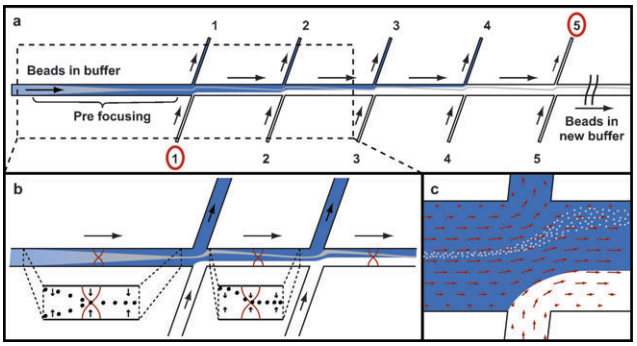

Fig. 12 Side-washing chip.[90] Beads in buffer enter the system and are focused in a band in the middle of the channel. At junction 1 the particle band will be displaced towards the upper wall because of the addition of clean buffer. The acoustic radiation force will however realign the particles in the middle and the cycle is repeated until the entire original medium has been shifted out and the beads are re-suspended in clean medium. With kind permission from Springer Science & Business Media, *Microchimica Acta*, Buffer medium exchange in continuous cell and particle streams using ultrasonic standing wave focusing, 2009, **164**, 269–277, Augustsson *et al.*, Fig. 3.

Augustsson *et al.* and showed a striking wash efficiency of 99.995%.[88] They also showed an application for phosphopeptide affinity extraction and sample preparation for mass spectrometry. Further work with the sequential medium exchange chip has involved affinity specific extraction of phage particles from phage display libraries.[89] Microbeads coated with a selected antigen were used to extract phages with a specific binding for the targeted antigen from a vast library of bacteriophages. Acoustic forces pulled the antigen beads with bound bacteriophages from the complex bead/phage library mixture into the clean buffer in the channel centre, Fig. 11. The enhanced medium exchange chip proved to be at least as efficient as conventional magnetic bead based separation approaches undergoing three washing steps and thus a much faster library selection procedure was demonstrated as compared to magnetic bead standards.

An alternative method to exchange the buffer medium is the so called side-washer chip.[90] The original buffer is translated sideways across the channel by the addition of clean buffer along the channel while the acoustic radiation force retains the beads aligned in the channel, Fig. 12. Although the band of focused beads gets slightly displaced every time new clean buffer is added, the acoustic radiation force refocuses the beads. Each junction has an exchange rate of 25% of the main buffer flow resulting in the buffer injected at inlet 1 will end up in outlet 5, red circles Fig. 12. The chip had eight cross-flow junctions and each junction increase the buffer exchange ratio accordingly. Wash efficiencies up to 96.4% were accomplished with a 0.2% solid content bead suspension, using eight cross-flow junctions, effectively exchanging the carrier buffer twice.

An alternative use of the side-washer was presented by Augustsson *et al.* where the cross-flow channels were not used for washing buffer but instead each branch injected a pH-buffer of varying degree.[91] This enabled the use of microbeads with ion-exchange properties and different surface bound peptides to be eluted from the beads during sequential

exposure to higher pH in the channel. The advantages of such a chip include the ability to perform multiplex probing on a single bead suspension at the same time as wash of contaminating background is performed and thereby increasing the detection limit in the subsequent mass spectrometry readout of the eluted peptides.

Continuous particle separation using surface acoustic standing waves (SAW) have also recently been reported.[92] The surface acoustic waves were generated using low power interdigital transducers microfabricated on the surface of a piezoelectric substrate. The separation channels were made in PDMS, a material which normally is not favourable when using the bulk acoustic techniques reported above, since it absorbs the acoustic energy effectively preventing the formation of a standing wave. However, in the SAW case, the acoustic energy was transferred to the suspension since the piezoelectric substrate acted as one of the channel walls, which meant that the acoustic wave was not attenuated while passing through a polymer. Surface acoustic waves have also recently been utilised to induce lateral acoustic streaming across the channel width and thus enables sideways translation of cells in front of a flow splitter such that desired cells are deviated into a collection output.[93]

Passive separation

There are devices, which do not utilize external forces for sorting or separation but rely purely on microfluidic phenomena and the interaction of the fluid with the geometries of the microfluidic chip.

Obstacle induced separation

Pinches, weirs and posts are common microfluidic obstacle components which are arranged in microfluidic channels to act as filters, preventing particles from entering certain areas. However, obstacles are not only used to filter cells or particles, but can also be used to alter fluid streamlines and particle trajectories.

Deterministic lateral displacement, DLD, is a method which utilizes micro post arrays arranged in micro channels to accomplish size separation of particles or cells.[94] A matrix of symmetrical posts or obstacles is fabricated in the channel such that the placement of each column of posts in the matrix post is shifted a short distance sideways relative the previous post column. Depending on the size of the particle, it will be deflected towards a neighbouring flow stream as it passes between two posts and will thus display a sideways displacement in its course through the post array. The trajectory is dependent on the asymmetry of the array. The distance a post is shifted, δ, and the total distance between two posts G, will determine how many streamlines the separator will have, see Fig. 13A. The number of streamlines will also limit the number of particle sizes that can be separated at the same time. The angle α of which particles will be deflected depends on the distance between the posts along the flow path, and can be calculated as $\tan^{-1}(\delta/\lambda)$, Fig. 13B. More detailed theoretical models for deterministic lateral displacement were developed by Inglis *et al.*[95]

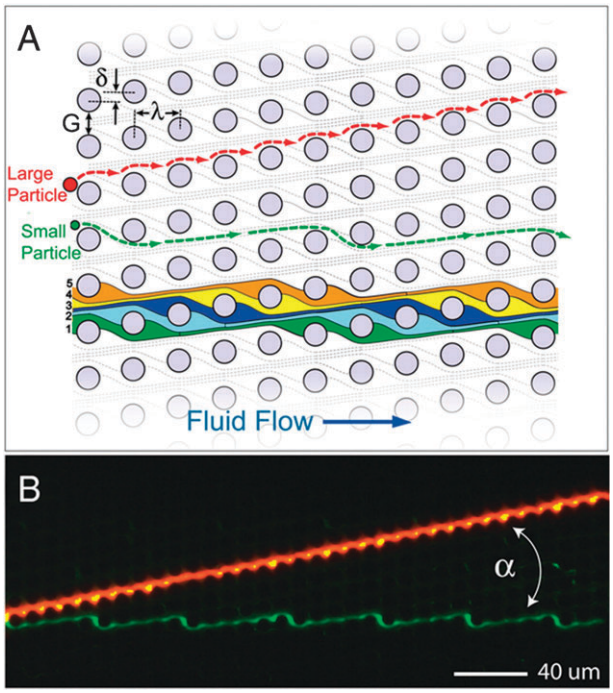

Fig. 13 Deterministic lateral displacement. The asymmetrical placements of the posts in the array cause particles of different sizes to follow different flow paths. This results in an in lateral displacement and thus separation of particles by size. Printed with permission from Morton *et al.*[96] Copyright 2008 National Academy of Sciences, USA.

Several different post combinations were investigated by Morton *et al.*, drawing parallels to optical phenomena as refraction and deflection as well as focusing particles into jets.[96] It was also shown that DLD enables the deflection of differently sized particles across laminar flows in the post array, which was utilized to fractionate *E. coli* cells and then subsequently direct the cells into another flow line containing cell-lysing solution.[97] The intracellular content was then further separated by the DLD and the DNA recovered. Recent developments in deterministic lateral displacement particle separation made by Beech *et al.* have shown bumper arrays that were tuneable with regards to the dynamic range of the particle sizing.[98] This was accomplished by the manufacturing of the bumper array in PDMS, which when stretched, displayed slightly rearranged post array geometries and thus altered separation characteristics. The same group later also demonstrated a combination of a bumper array with dielectrophoresis to accomplish a separation system with increased dimensionality.[99]

A related technique which relies on obstacles is the *Brownian ratchet* based separators. In contrast to deterministic lateral displacement, Brownian ratchets are comprised of asymmetrical posts in a symmetric array.[100] The ratchet will only work on small particles, such as macromolecules, which are affected by Brownian motion. As a suspended mixture of particles flow through the ratchet they will bump into slanted obstacles which will deflect their trajectories. They will however also experience a lateral movement due to diffusion. Small particles will move farther by Brownian diffusion than larger ones and are therefore more likely to move further sideways.

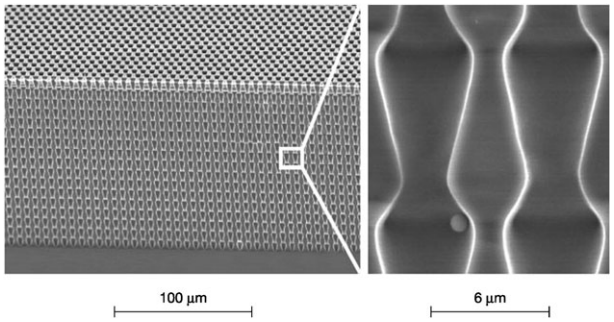

Fig. 14 Cross-section SEM image of a macro porous silicon membrane designed as a massively parallel ratchet. Reprinted by permission from Macmillan Publishers Ltd, *Nature*,[104] copyright 2003.

The Brownian ratchet will thus separate by size in a lateral direction. The geometry of the posts and the distance between them influences the mechanism and separation degree and have to be considered when designing the ratchet.[101] Since only very small particles can be used, DNA molecules have proven very suitable to separate.[102] A system with a precisely controlled injection scheme, developed by Cabodi *et al.*, allowed separation of two different DNA molecules into their respective components.[103] An interesting design to accomplish a substantial up scaling of the separation throughput was demonstrated by Matthias and Müller using a massively parallel Brownian ratchet realised as asymmetric pores in a silicon membrane, Fig. 14.[104]

A technique similar to the obstacle arrays is the *hydrophoretic separation*.[105] The chip is comprised of a channel with slanted objects as obstacles placed at the top and bottom of the channel in an alternating fashion. The slanted objects create local transverse flows perpendicular to the direction of the main flow. Particles were thus transported from one sidewall of the channel to the other. The combination of the hydrophoretic separation with a vertical weir placed in the pathway of the lined up particles, enabled size fractionation as the larger particles did not pass through the narrow gap but instead followed the obstacle to a larger gap at the other side wall of the channel. Utilizing this device Choi *et al.* were able to separate white blood cells from red with an enrichment ratio of ~210-fold at a throughput of 4×10^3 cells s^{-1}.[106]

Hydrodynamic filtration

Hydrodynamic filtration is a principle which is similar to cross flow filtration which utilizes small capillary branches perpendicular to the main flow. However, in cross flow filtration the entrance to the side branches is made either very narrow such that particles or cells are prevented to enter the channel, or large enough for particles of a certain size to pass. A common application of the cross flow filtration is to extract plasma from blood and the perpendicular side branches solves the problem of saturation as would be the problem of an ordinary membrane filter.[107–109] In hydrodynamic filtration, the main purpose of the side branches is not only to remove carrier fluid, but they also force particles to move closer the side walls of the main channel.[110] The side branches contain no contraction and are wider than the particle diameters. The precise control of the flow of the side branches decides which

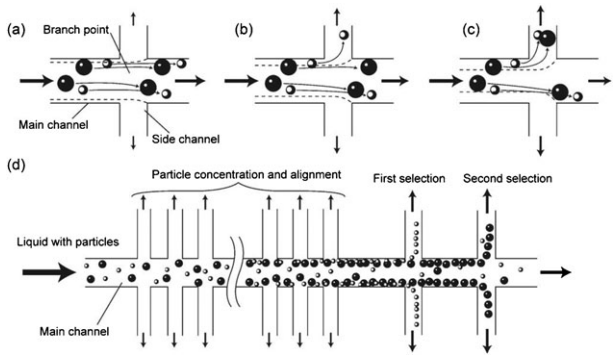

Fig. 15 The principle of hydrodynamic filtration. Excess fluid is removed gradually from the side branches perpendicular to the main flow. This action will eventually line up particles along the main channel walls. By controlling the flow rate of the side branch flow it is possible to remove particle fractions of a particular size while larger particle moves on to be separated later. From Yamada and Seki.[110] Reproduced by permission of the Royal Society of Chemistry.

fractions will be removed, as illustrated in Fig. 15. When the relative flow rate in the side channels is low (a), no particles will be diverted to the side branches—only fluid. In (b), medium flow rate is applied to the side channels allowing small particles to be separated with the medium but not large particles as these have a hydrodynamic centre line outside the dashed flow line that diverts into the side branch, while in (c) relative high flow rates to the side will not result in any particle separation. The dashed lines in Fig. 15a–c show the virtual boundaries of the layers of fluid in the main channel that will be diverted into the side branches. Before the separation branches there are multiple branches responsible for aligning and concentrating the particles along the side walls by medium removal.

The technique has also been demonstrated in the separation of white blood cells (WBC) from red blood cells (RBC). An alternate design providing improved particle alignment prior to the hydrodynamic separation was also developed where the carrier medium fractions removed during the alignment process were recombined with the main flow.[111] By adding extra inlets perpendicular to the flow, carrier-medium exchange is performed in several steps, providing an aspiration and washing procedure for continuous flow cell processing.[112]

A related effect which can be used to separate particles or cells from their medium is the Zweifach-Fung effect. It states that a suspension flowing through a bifurcation, where the branches have different cross sections or flow rates, the particles are prone to follow the branch of the higher flow rate while particle free medium exits through the branch of lower flow rate. A common application for this technique is to separate cell free plasma from blood.[113] Fan *et al.* combined the plasmapheresis chip with a DNA-encoded antibody library (DEAL) technique for multiplexed analysis of proteins in the plasma.[114] The DEAL array was patterned in a barcode style in the plasma channels which enabled easy readout of the detected proteins.

Blood plasma is a particularly favourable for separation as the blood cells tend to migrate into the centre of a microfluidic channel leaving a seam of plasma at the channel boundaries.

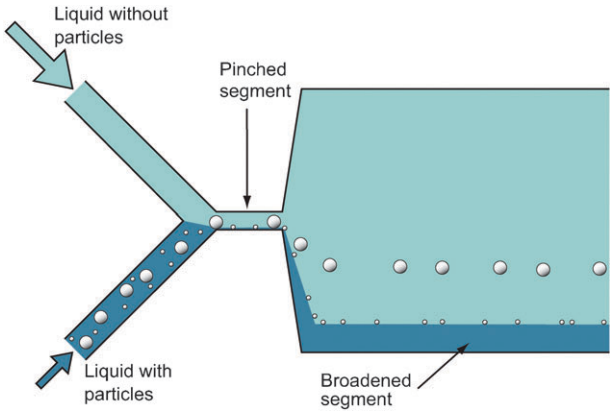

Fig. 16 Principle of pinched flow fractionation. Particles in a suspension are focused along the side wall in a pinched segment with a clean buffer. As they enter the expansion chamber the broadening of the laminar streamlines separate the particles by size.

By using channels perpendicular to the main flow it is possible to harvest the cell free plasma (plasma skimming).[115]

Pinched flow fractionation

In pinched flow fractionation, two inlets are used; one which contains a particle suspension with particles of different sizes and one particle free buffer. The buffer flows at a higher rate and laminates the particles in the other suspension to one sidewall in the pinching region, regardless of particle size. The particles are pinched to the side wall with a centre line at a distance equal to their radius and move along streamlines that pass through their hydrodynamic centres. As the particles enter the expansion chamber, the laminar streamlines are expanded and the particles are separated perpendicularly to the flow direction according to their sizes, see Fig. 16.

The expansion chamber is then split into multiple outlets collecting the fractionated particles. The basic principle was shown by Yamada *et al.*[116] and an improved device with asymmetrically arranged separation branches have also been developed.[117,118] Further enhancement including flow rate control valves[119] as well as replacing the pressure driven flow with EOF has been reported.[120]

Inertia and Dean flow

Inertial lift forces, sometimes called wall effect forces, have recently been used in numerous microfluidic applications. The lift forces induce migration of particles between streamlines in the laminar flow entraining them at a specific lateral position where the wall lift force and the force of the shear gradient of the flow are at equilibrium.[121] In a circular flow channel particles create an annulus and in a channel of rectangular cross-section they end up at equilibrium positions along the centre of each side. Di Carlo *et al.* used a symmetric and an asymmetric channel in a meander fashion to line up particles.[122] By using flow splitters it is possible to concentrate or separate the particle streams. Since the lift force on a particle is size dependent, different sized particles will end up in different streamlines after reaching equilibrium, thus enabling size fractionation.[123] Park *et al.* also used the lift force to affect particles in suspension in a device which consisted of a series of expanding and contracting rectangular channels.[124] The difference in cross-section of the channel induced vortices which further facilitated the migration of the particles and eventually gathered them into two streams.

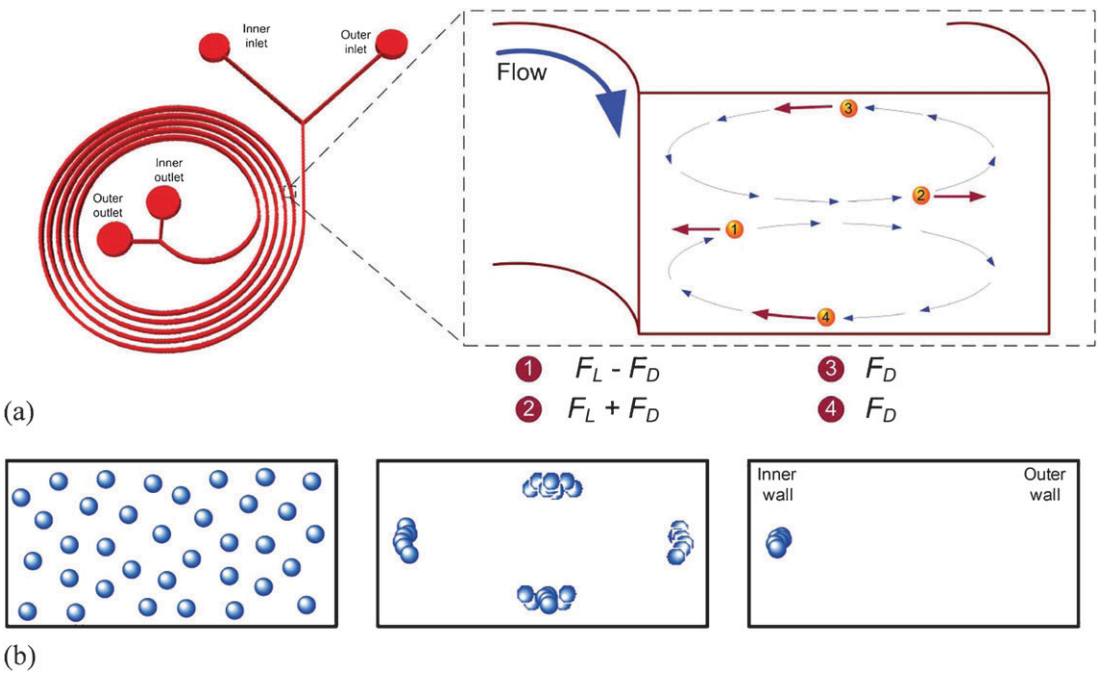

Fig. 17 The spiral separator consists of two inlets and two outlets with the sample being introduced through the inner inlet. Neutrally buoyant particles experience lift forces (F_L) and Dean drag (F_D), which results in differential particle migration within the microchannel. The lift forces positions particles into four different equilibrium positions and additional forces by the Dean vortices reduce the four equilibrium positions into one close to the inner wall. From Bhagat *et al.*[125] Reproduced by permission of the Royal Society of Chemistry.

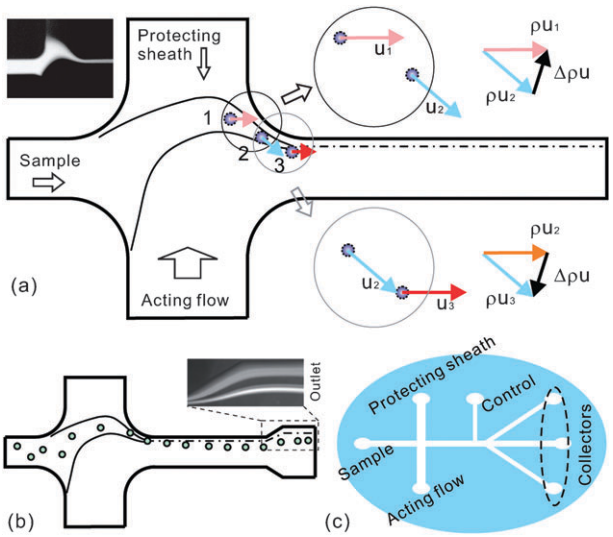

Fig. 18 Soft inertial microfluidics utilized by Wu *et al.* to separate bacteria from human blood cells.[130] The curved flow caused by careful flow control results in a larger inertial force on the cells separation them from the smaller bacteria. Reproduced by permission of the Royal Society of Chemistry.

Curved channels generate a secondary flow which arises from a mismatch in velocity between the fluid in the centre and the near-wall regions of a channel. Central fluid elements have larger inertia than fluid elements at the walls and would tend to flow outward around a curve creating pressure gradient along the curve. This pressure gradient causes the relatively stagnant fluid near the wall to circulate creating two symmetrical vortices. These vortices are known as Dean vortices.[126] The secondary flow further reduces the four equilibrium positions made by lift forces to only one position near the inner wall, see Fig. 17b.[125] This is the case of larger particles in a curved channel, smaller particles, however, migrate to the outer half of the channel under the influence of the Dean forces. This enables a size separation where large and small particles end up in two distinct particle streams.[127] Bhagat *et al.* used a curved channel of rectangular cross-section to separate 1.9 μm beads from 7.32 μm beads. They also showed a successful separation of 590 nm nanoparticles from 1.9 μm particles.[128] The aspect ratio of the curved channel, *i.e.* the height/width relationship, also seems to affect the positions of particles of different sizes. Russom *et al.* showed that different sized particles find equilibrium at different heights in the curved channel.[129] Inertial forces was also used by Wu *et al.* to separate bacteria from human blood cells, Fig. 18.[130] An extra inlet providing an asymmetrical sheath flow together with the geometry of the inlets generated a soft inertial force on the sample fluid in the curved and focused sample flow segment which deflected larger particles, while the smaller ones were kept on or near the original flow streamline.

Conclusions

This review covers the major areas of research that targets cell handling and particle handling microsystems in a continuous flow mode. The combination of bead or cell based assays and laminar flow in lab-on-a-chip systems together with intrinsically or externally generated forces opens up a vast variety of opportunities to design advanced protocols for cell and particle handling as reviewed herein. The rapid increase in scientific efforts along this line holds promise for the future of improved flow cytometry systems in both preclinical research and development as well as in forth coming systems for advanced cytometry diagnostics and potentially also as modalities for next generation cell based therapeutics. Critical aspects will be system robustness, *i.e.* being able to process biological samples from a broad patient cohort under identical conditions with satisfactory performance. Also, the ability to process sufficient number of cells per time unit as well as being able to process whole blood or modestly diluted whole blood are requirements that future developments will have to address.

Acknowledgements

Vinnova programme: Innovation for Future Health—Cell CARE, The Swedish Research Council Project no:s. 2006–7600, 2007–4946, Foundation for Strategic Research, Crafoordstiftelsen, Carl Trygger Foundation, Royal Physiographic Society in Lund, and Knut & Alice Wallenberg Foundation are greatly acknowledged for their financial support.

References

1 H. R. Hulett, W. A. Bonner, J. Barrett and L. A. Herzenberg, *Science*, 1969, **166**, 747–749.
2 W. A. Bonner, R. G. Sweet, H. R. Hulett and L. A. Herzenberg, *Rev. Sci. Instrum.*, 1972, **43**, 404–409.
3 M. H. Julius, E. Simpson and L. A. Herzenberg, *Eur. J. Immunol.*, 1973, **3**, 645–649.
4 US Pat., 2 656 508, 1953.
5 S. Gawad, L. Schild and P. Renaud, *Lab Chip*, 2001, **1**, 76–82.
6 J. Zhe, A. Jagtiani, P. Dutta, J. Hu and J. Carletta, *J. Micromech. Microeng.*, 2007, **17**, 304–313.
7 T. Sun, D. Holmes, S. Gawad, N. G. Green and H. Morgan, *Lab Chip*, 2007, **7**, 1034–1040.
8 D. Holmes, D. Pettigrew, C. H. Reccius, J. D. Gwyer, C. van Berkel, J. Holloway, D. E. Davies and H. Morgan, *Lab Chip*, 2009, **9**, 2881–2889.
9 A. Y. Fu, C. Spence, A. Scherer, F. H. Arnold and S. R. Quake, *Nat. Biotechnol.*, 1999, **17**, 1109–1111.
10 J. Kruger, K. Singh, A. O'Neill, C. Jackson, A. Morrison and P. O'Brien, *J. Micromech. Microeng.*, 2002, **12**, 486–494.
11 M. M. Wang, E. Tu, D. E. Raymond, J. M. Yang, H. C. Zhang, N. Hagen, B. Dees, E. M. Mercer, A. H. Forster, I. Kariv, P. J. Marchand and W. F. Butler, *Nat. Biotechnol.*, 2005, **23**, 83–87.
12 D. Holmes, H. Morgan and N. G. Green, *Biosens. Bioelectron.*, 2006, **21**, 1621–1630.
13 J. El-Ali, P. K. Sorger and K. F. Jensen, *Nature*, 2006, **442**, 403–411.
14 J. Nilsson, M. Evander, B. Hammarstrom and T. Laurell, *Anal. Chim. Acta*, 2009, **649**, 141–157.
15 N. Pamme, *Lab Chip*, 2007, **7**, 1644–1659.
16 S. Miltenyi, W. Muller, W. Weichel and A. Radbruch, *Cytometry*, 1990, **11**, 231–238.
17 I. Safarik and M. Safarikova, *J. Chromatogr., B: Biomed. Sci. Appl.*, 1999, **722**, 33–53.
18 J. C. Giddings, *Sep. Sci. Technol.*, 1966, **1**, 123.
19 K. D. Caldwell, J. C. Giddings, M. N. Myers and L. F. Kesner, *Science*, 1972, **176**, 296-&.

20 G. H. Thompson, M. N. Myers and J. C. Giddings, *Anal. Chem.*, 1969, **41**, 1219-&.
21 P. J. P. Cardot, J. Gerota and M. Martin, *J. Chromatogr., B: Biomed. Sci. Appl.*, 1991, **568**, 93–103.
22 J. C. Giddings, F. J. F. Yang and M. N. Myers, *Science*, 1976, **193**, 1244–1245.
23 S. K. R. Williams and D. Lee, *J. Sep. Sci.*, 2006, **29**, 1720–1732.
24 F. A. Messaud, R. D. Sanderson, J. R. Runyon, T. Otte, H. Pasch and S. K. R. Williams, *Prog. Polym. Sci.*, 2009, **34**, 351–368.
25 B. Roda, A. Zattoni, P. Reschiglian, M. H. Moon, M. Mirasoli, E. Michelini and A. Roda, *Anal. Chim. Acta*, 2009, **635**, 132–143.
26 J. C. Giddings, *J. Chem. Educ.*, 1973, **50**, 667–669.
27 K. D. Caldwell, Z. Q. Cheng, P. Hradecky and J. C. Giddings, *Cell Biophysics*, 1984, **6**, 233–251.
28 J. C. Giddings, *Sep. Sci. Technol.*, 1983, **18**, 765–773.
29 J. C. Giddings, *Sep. Sci. Technol.*, 1985, **20**, 749–768.
30 J. J. Lai, K. E. Nelson, M. A. Nash, A. S. Hoffman, P. Yager and P. S. Stayton, *Lab Chip*, 2009, **9**, 1997–2002.
31 U. Kim, C. W. Shu, K. Y. Dane, P. S. Daugherty, J. Y. J. Wang and H. T. Soh, *Proc. Natl. Acad. Sci. U. S. A.*, 2007, **104**, 20708–20712.
32 D. Huh, J. H. Bahng, Y. B. Ling, H. H. Wei, O. D. Kripfgans, J. B. Fowlkes, J. B. Grotberg and S. Takayama, *Anal. Chem.*, 2007, **79**, 1369–1376.
33 J. J. Hawkes, R. W. Barber, D. R. Emerson and W. T. Coakley, *Lab Chip*, 2004, **4**, 446–452.
34 M. A. M. Gijs, *Microfluid. Nanofluid.*, 2004, **1**, 22–40.
35 Q. A. Pankhurst, J. Connolly, S. K. Jones and J. Dobson, *J. Phys. D: Appl. Phys.*, 2003, **36**, R167–R181.
36 N. Pamme and A. Manz, *Anal. Chem.*, 2004, **76**, 7250–7256.
37 S. A. Peyman, A. Iles and N. Pamme, *Chem. Commun.*, 2008, 1220–1222.
38 C. Carr, M. Espy, P. Nath, S. L. Martin, M. D. Ward and J. Martin, *J. Magn. Magn. Mater.*, 2009, **321**, 1440–1445.
39 J. D. Adams, U. Kim and H. T. Soh, *Proc. Natl. Acad. Sci. U. S. A.*, 2008, **105**, 18165–18170.
40 X. H. Lou, J. R. Qian, Y. Xiao, L. Viel, A. E. Gerdon, E. T. Lagally, P. Atzberger, T. M. Tarasow, A. J. Heeger and H. T. Soh, *Proc. Natl. Acad. Sci. U. S. A.*, 2009, **106**, 2989–2994.
41 C. W. Yung, J. Fiering, A. J. Mueller and D. E. Ingber, *Lab Chip*, 2009, **9**, 1171–1177.
42 N. Pamme, *Lab Chip*, 2006, **6**, 24–38.
43 E. P. Furlani, *J. Phys. D: Appl. Phys.*, 2007, **40**, 1313–1319.
44 K. H. Han and A. B. Frazier, *J. Appl. Phys.*, 2004, **96**, 5797–5802.
45 J. H. Kang, S. Choi, W. Lee and J. K. Park, *J. Am. Chem. Soc.*, 2008, **130**, 396–397.
46 A. Ashkin, *Phys. Rev. Lett.*, 1970, **24**, 156-&.
47 A. Ashkin, J. M. Dziedzic, J. E. Bjorkholm and S. Chu, *Opt. Lett.*, 1986, **11**, 288–290.
48 J. E. Molloy and M. J. Padgett, *Contemp. Phys.*, 2002, **43**, 241–258.
49 K. Dholakia, P. Reece and M. Gu, *Chem. Soc. Rev.*, 2008, **37**, 42–55.
50 A. Ashkin and J. M. Dziedzic, *Science*, 1987, **3–235**, 1517–1520.
51 M. P. MacDonald, G. C. Spalding and K. Dholakia, *Nature*, 2003, **426**, 421–424.
52 A. Jonas and P. Zemanek, *Electrophoresis*, 2008, **29**, 4813–4851.
53 T. D. Perroud, J. N. Kaiser, J. C. Sy, T. W. Lane, C. S. Branda, A. K. Singh and K. D. Patel, *Anal. Chem.*, 2008, **80**, 6365–6372.
54 K. Ladavac, K. Kasza and D. G. Grier, *Phys. Rev. E: Stat., Nonlinear, Soft Matter Phys.*, 2004, **70**, 010901.
55 H. A. Pohl, *J. Appl. Phys.*, 1951, **22**, 869–871.
56 J. Voldman, *Annu. Rev. Biomed. Eng.*, 2006, **8**, 425–454.
57 S. Fiedler, S. G. Shirley, T. Schnelle and G. Fuhr, *Anal. Chem.*, 1998, **70**, 1909–1915.
58 P. R. C. Gascoyne and J. Vykoukal, *Electrophoresis*, 2002, **23**, 1973–1983.
59 L. Wang, J. Lu, S. A. Marukenko, E. S. Monuki, L. A. Flanagan and A. P. Lee, *Electrophoresis*, 2009, **30**, 782–791.
60 C. F. Gonzalez and V. T. Remcho, *J. Chromatogr., A*, 2005, **1079**, 59–68.
61 E. B. Cummings and A. K. Singh, *Anal. Chem.*, 2003, **75**, 4724–4731.
62 L. M. Barrett, A. J. Skulan, A. K. Singh, E. B. Cummings and G. J. Fiechtner, *Anal. Chem.*, 2005, **77**, 6798–6804.
63 Y. Huang, K. L. Ewalt, M. Tirado, R. Haigis, A. Forster, D. Ackley, M. J. Heller, J. P. O Connell and M. Krihak, *Anal. Chem.*, 2001, **73**, 1549–1559.
64 U. Kim, J. R. Qian, S. A. Kenrick, P. S. Daugherty and H. T. Soh, *Anal. Chem.*, 2008, **80**, 8656–8661.
65 M. S. Pommer, Y. T. Zhang, N. Keerthi, D. Chen, J. A. Thomson, C. D. Meinhart and H. T. Soh, *Electrophoresis*, 2008, **29**, 1213–1218.
66 H. H. Cui, J. Voldman, X. F. He and K. M. Lim, *Lab Chip*, 2009, **9**, 2306–2312.
67 M. D. Vahey and J. Voldman, *Anal. Chem.*, 2008, **80**, 3135–3143.
68 N. Gadish and J. Voldman, *Anal. Chem.*, 2006, **78**, 7870–7876.
69 I. Doh and Y. H. Cho, *Sens. Actuators, A*, 2005, **121**, 59–65.
70 T. Braschler, N. Demierre, E. Nascimento, T. Silva, A. G. Oliva and P. Renaud, *Lab Chip*, 2008, **8**, 280–286.
71 R. L. Tornay, T. Braschler, N. Demierre, B. Steitz, A. Finka, H. Hofmann, J. A. Hubbell and P. Renaud, *Lab Chip*, 2008, **8**, 267–273.
72 T. Laurell, F. Petersson and A. Nilsson, *Chem. Soc. Rev.*, 2007, **36**, 492–506.
73 F. Petersson, A. Nilsson, C. Holm, H. Jonsson and T. Laurell, *Analyst*, 2004, **129**, 938–943.
74 M. Evander, A. Lenshof, T. Laurell and J. Nilsson, *Anal. Chem.*, 2008, **80**, 5178–5185.
75 C. Grenvall, M. Carlsson, P. Augustsson, F. Petersson and T. Laurell, *Proceedings of the 11th International Conference on Micro Total Analysis Systems*, Paris, France, 2007.
76 A. Nilsson, F. Petersson, H. Jonsson and T. Laurell, *Lab Chip*, 2004, **4**, 131–135.
77 S. M. Hagsater, A. Lenshof, P. Skafte-Pedersen, J. P. Kutter, T. Laurell and H. Bruus, *Lab Chip*, 2008, **8**, 1178–1184.
78 N. R. Harris, M. Hill, S. Beeby, Y. Shen, N. M. White, J. J. Hawkes and W. T. Coakley, *Sens. Actuators, B*, 2003, **95**, 425–434.
79 A. Lenshof, A. Ahmad-Tajudin, K. Jaras, A. M. Sward-Nilsson, L. Aberg, G. Marko-Varga, J. Malm, H. Lilja and T. Laurell, *Anal. Chem.*, 2009, **81**, 6030–6037.
80 H. Jonsson, C. Holm, A. Nilsson, F. Petersson, P. Johnsson and T. Laurell, *Ann. Thorac. Surg.*, 2004, **78**, 1572–1578.
81 C. Grenvall, P. Augustsson, J. R. Folkenberg and T. Laurell, *Anal. Chem.*, 2009, **81**, 6195–6200.
82 F. Petersson, L. Aberg, A. M. Sward-Nilsson and T. Laurell, *Anal. Chem.*, 2007, **79**, 5117–5123.
83 M. Evander, L. Johansson, T. Lilliehorn, J. Piskur, M. Lindvall, S. Johansson, M. Almqvist, T. Laurell and J. Nilsson, *Anal. Chem.*, 2007, **79**, 2984–2991.
84 J. Hultstrom, O. Manneberg, K. Dopf, H. M. Hertz, H. Brismar and M. Wiklund, *Ultrasound Med. Biol.*, 2007, **33**, 145–151.
85 D. Bazou, W. T. Coakley, A. J. Hayes and S. K. Jackson, *Toxicol. in Vitro*, 2008, **22**, 1321–1331.
86 L. Johansson, F. Nikolajeff, S. Johansson and S. Thorslund, *Anal. Chem.*, 2009, **81**, 5188–5196.
87 F. Petersson, A. Nilsson, H. Jonsson and T. Laurell, *Anal. Chem.*, 2005, **77**, 1216–1221.
88 P. Augustsson, J. Persson, S. Ekstrom, M. Ohlin and T. Laurell, *Lab Chip*, 2009, **9**, 810–818.
89 J. Persson, P. Augustsson, T. Laurell and M. Ohlin, *FEBS J.*, 2008, **275**, 5657–5666.
90 P. Augustsson, L. B. Aberg, A. M. K. Sward-Nilsson and T. Laurell, *Microchim. Acta*, 2009, **164**, 269–277.
91 P. Augustsson, T. Laurell and S. Ekström, *Proceedings of the 12th International Conference on Micro Total Analysis Systems*, San Diego, CA, USA, 2008.
92 J. J. Shi, H. Huang, Z. Stratton, Y. P. Huang and T. J. Huang, *Lab Chip*, 2009, **9**, 3354–3359.
93 T. Franke, S. Braunmüller, L. Schmid, A. Wixforth and D. A. Weitz, *Lab Chip*, 2010, DOI: 10.1039/b915522h.
94 L. R. Huang, E. C. Cox, R. H. Austin and J. C. Sturm, *Science*, 2004, **304**, 987–990.
95 D. W. Inglis, J. A. Davis, R. H. Austin and J. C. Sturm, *Lab Chip*, 2006, **6**, 655–658.
96 K. J. Morton, K. Loutherback, D. W. Inglis, O. K. Tsui, J. C. Sturm, S. Y. Chou and R. H. Austin, *Proc. Natl. Acad. Sci. U. S. A.*, 2008, **105**, 7434–7438.

97 K. J. Morton, K. Loutherback, D. W. Inglis, O. K. Tsui, J. C. Sturm, S. Y. Chou and R. H. Austin, *Lab Chip*, 2008, **8**, 1448–1453.
98 J. P. Beech and J. O. Tegenfeldt, *Lab Chip*, 2008, **8**, 657–659.
99 J. P. Beech, P. Jonsson and J. O. Tegenfeldt, *Lab Chip*, 2009, **9**, 2698–2706.
100 T. A. J. Duke and R. H. Austin, *Phys. Rev. Lett.*, 1998, **80**, 1552–1555.
101 L. R. Huang, P. Silberzan, J. O. Tegenfeldt, E. C. Cox, J. C. Sturm, R. H. Austin and H. Craighead, *Phys. Rev. Lett.*, 2002, **89**, 178301.
102 C. F. Chou, O. Bakajin, S. W. P. Turner, T. A. J. Duke, S. S. Chan, E. C. Cox, H. G. Craighead and R. H. Austin, *Proc. Natl. Acad. Sci. U. S. A.*, 1999, **96**, 13762–13765.
103 M. Cabodi, Y. F. Chen, S. W. P. Turner, H. G. Craighead and R. H. Austin, *Electrophoresis*, 2002, **23**, 3496–3503.
104 S. Matthias and F. Muller, *Nature*, 2003, **424**, 53–57.
105 S. Choi and J. K. Park, *Lab Chip*, 2007, **7**, 890–897.
106 S. Choi, S. Song, C. Choi and J. K. Park, *Lab Chip*, 2007, **7**, 1532–1538.
107 T. A. Crowley and V. Pizziconi, *Lab Chip*, 2005, **5**, 922–929.
108 V. VanDelinder and A. Groisman, *Anal. Chem.*, 2006, **78**, 3765–3771.
109 E. Sollier, H. Rostaing, P. Pouteau, Y. Fouillet and J. L. Achard, *Sens. Actuators, B*, 2009, **141**, 617–624.
110 M. Yamada and M. Seki, *Lab Chip*, 2005, **5**, 1233–1239.
111 M. Yamada and M. Seki, *Anal. Chem.*, 2006, **78**, 1357–1362.
112 M. Yamada, J. Kobayashi, M. Yamato, M. Seki and T. Okano, *Lab Chip*, 2008, **8**, 772–778.
113 S. Yang, A. Undar and J. D. Zahn, *Lab Chip*, 2006, **6**, 871–880.
114 R. Fan, O. Vermesh, A. Srivastava, B. K. H. Yen, L. D. Qin, H. Ahmad, G. A. Kwong, C. C. Liu, J. Gould, L. Hood and J. R. Heath, *Nat. Biotechnol.*, 2008, **26**, 1373–1378.
115 R. D. Jaggi, R. Sandoz and C. S. Effenhauser, *Microfluid. Nanofluid.*, 2007, **3**, 47–53.
116 M. Yamada, M. Nakashima and M. Seki, *Anal. Chem.*, 2004, **76**, 5465–5471.
117 J. Takagi, M. Yamada, M. Yasuda and M. Seki, *Lab Chip*, 2005, **5**, 778–784.
118 X. L. Zhang, J. M. Cooper, P. B. Monaghan and S. J. Haswell, *Lab Chip*, 2006, **6**, 561–566.
119 Y. Sai, M. Yamada, M. Yasuda and M. Seki, *J. Chromatogr., A*, 2006, **1127**, 214–220.
120 T. Kawamata, M. Yamada, M. Yasuda and M. Seki, *Electrophoresis*, 2008, **29**, 1423–1430.
121 D. Di Carlo, *Lab Chip*, 2009, **9**, 3038–3046.
122 D. Di Carlo, D. Irimia, R. G. Tompkins and M. Toner, *Proc. Natl. Acad. Sci. U. S. A.*, 2007, **104**, 18892–18897.
123 D. Di Carlo, J. F. Edd, D. Irimia, R. G. Tompkins and M. Toner, *Anal. Chem.*, 2008, **80**, 2204–2211.
124 J. S. Park, S. H. Song and H. I. Jung, *Lab Chip*, 2009, **9**, 939–948.
125 A. A. S. Bhagat, S. S. Kuntaegowdanahalli and I. Papautsky, *Lab Chip*, 2008, **8**, 1906–1914.
126 T. M. Squires and S. R. Quake, *Rev. Mod. Phys.*, 2005, **77**, 977–1026.
127 D. H. Yoon, J. B. Ha, Y. K. Bahk, T. Arakawa, S. Shoji and J. S. Go, *Lab Chip*, 2009, **9**, 87–90.
128 A. A. S. Bhagat, S. S. Kuntaegowdanahalli and I. Papautsky, *Microfluid. Nanofluid.*, 2009, **7**, 217–226.
129 A. Russom, A. K. Gupta, S. Nagrath, D. Di Carlo, J. F. Edd and M. Toner, *New J. Phys.*, 2009, **11**, 075025.
130 Z. G. Wu, B. Willing, J. Bjerketorp, J. K. Jansson and K. Hjort, *Lab Chip*, 2009, **9**, 1193–1199.